THE IMPORTANCE OF THE MUON SPIN ROTATION (μSR) TECHNIQUE IN LOW TEMPERATURE PHYSICS

A. Schenck

JOURNAL DE PHYSIQUE Colloque C6, supplément au n° 8, Tome 39, août 1978, page C6-1478

THE IMPORTANCE OF THE MUON SPIN ROTATION (μSR) TECHNIQUE IN LOW TEMPERATURE PHYSICS

A. Schenck

Laboratory for High Energy Physics, Swiss Federal Institute of Technology (ETH), Zürich, c/o SIN, CH-5234 Villigen, Switzerland

Résumé.- En introduction, on présente les principes de la technique de rotation du spin muonique (μSR), suivis d'une revue des applications de cette méthode en physique des basses températures. L'accent est porté sur la diffusion des muons dans les métaux, dont les aspects constituent une variante de la diffusion de l'hydrogène. La possibilité d'étudier certains effets magnétiques accompagnant des transitions de phases dans des substances ferromagnétiques et antiferromagnétiques, des systèmes de verres de spins et de moments magnétiques géants, est également discutée.

Abstract.- An introduction to the principles of the μSR-technique will be given followed by a review of various applications of this method at "low" temperatures. The main emphasis will be placed on low temperature aspects of the diffusion of positive muons in metals as a particular variant of hydrogen diffusion, and on the possibilities of studying magnetic effects, accompanying phase transitions, in ferromagnets and antiferromagnets, in spin glasses and giant moment systems.

1. INTRODUCTION.- The Muon Spin Rotation (μSR) technique is being applied systematically to problems in solid state physics and chemistry since about 1970 /1,2/, although the principle idea of using positive muons as a probe is as old as the detection of parity violation in the muon decay in 1957, when it became apparent immediately that muons loose their spin polarization by interactions with the target environment /3/. With the advancement of the so called meson factories and the availability of intense muon beams the interest in the μSR method has grown steadily and there are by now groups from more than 25 institutions actively involved in μSR research at the accelerator laboratories of CERN, DUBNA, GATCHINA, TRIUMF, LAMPF, SREL and SIN.

As far as solid state physics is concerned one has tried to use positive muons on quite different subjects /4/. The bulk of the data were obtained from studies of the muon behavior in metals, concerning mobility, localization, trapping at impurities, electronic structure and muon-host lattice interactions /5/, and from the study of hyperfine fields and dipole fields in magnetic substances /6/. With regard to the first circle of topics the positive muon can be considered a light isotope of hydrogen, the mass ratio being $m_\mu/m_p \simeq 1/9$. By studying the behavior of muons in metals one is in fact studying the behavior of hydrogen in metals extended to a smaller mass region. This may give rise to very pronounced isotope effects which could be compared with theoretical predictions, for example with regard to the quantum nature of "hydrogen"-diffusion /7/.

The latter field of studies in magnetic materials has particularly created interest as it allows in principle the investigation of magnetic properties at interstitial sites, not accessible so easily, where the muon usually seems to reside /6/. Compared with other microscopic probes that measure in real space the muon does not possess a complicated electron core or no electron core in the usual sense at all. As one was forced to learn, however, the disturbing effects of the screened muon charge on the host lattice are considerable and only very involved many body calculations are able to properly describe the actual physics involved. Nevertheless in many cases, as we shall see furtherdown, it is not necessary to know about the detailed electronic structure of the muon and the perturbing effects on the lattice as certain magnetic properties are directly reflected in the muons message to the experimenter.

In the following we will first discuss the principles of the μSR-method and then go on to a presentation of various experiments first concerning muon diffusion, etc. in metals and secondly concerning the study of magnetic properties of ferromagnetic and antiferromagnetic substances, spin glasses and giant moment alloys. The emphasis will be in all cases on the "low temperature" aspects or aspects that could be important also in low temperature studies.

2. THE PRINCIPLES OF THE μSR-METHOD.- The muon (μ) is a weakly and electromagnetically interacting particle. Some of its properties are collected in table I. We will only be concerned with positive muons.

Table I : Properties of the muon.

Mass :	105.6595(3) MeV = 206.7684(6).m_e = 0.1126 . m_p
Charge :	+e , − e
Spin :	1/2
Mag. Moment :	$\mu_\mu = \frac{1}{2}\frac{e\hbar}{mc}\, g\, S_z$ = 3.1833448(29).μ_p
Gyromag. ratio :	γ_μ = 13.55 × 10^3 Hz/gauss
Average lifetime :	τ_μ = 2.1994(6) μs
Decay :	$\mu^+ \to e^+ + \nu_e + \bar{\nu}_\mu$ $\mu^- \to e^- + \bar{\nu}_e + \nu_\mu$
Angular distribution of e^+, e^- :	$dN_e \pm \cong (1 \pm A\cdot\cos\theta)\, d\Omega$ A ~ 0.3, θ = ∢ ($\vec{S}_\mu$, $\vec{P}_e$ ±)
Production :	$\pi^\pm \to \mu^\pm + \nu_\mu\ (\bar{\nu}_\mu)$ $\tau_\pi = 2.2 \times 10^{-8}$ s.

Due to parity violation in the muon decay the positrons will show an asymmetric distribution with respect to the muon spin. This together with the availability of spin polarized muon beams /8/ constitutes the prerequisites, on which the μSR-method is based.

The most widely used experimental arrangement is one in which an external magnetic field is applied perpendicular to the initial polarization vector, which is along the μ^+-beam axis (see figure 1). Stopped μ^+ will consequently start to precess with a frequency $\omega_\mu = 2\pi\, \gamma_\mu\, B_{ext}$. With the same frequency the asymmetric positron emission distribution will sweep past a positron detection telescope, positioned in the precession plane, giving rise to an oscillatory positron rate in this telescope as a function of muon life time in the target. The actual measurement consists in starting a clock with a stopped muon signal, stopping the clock with

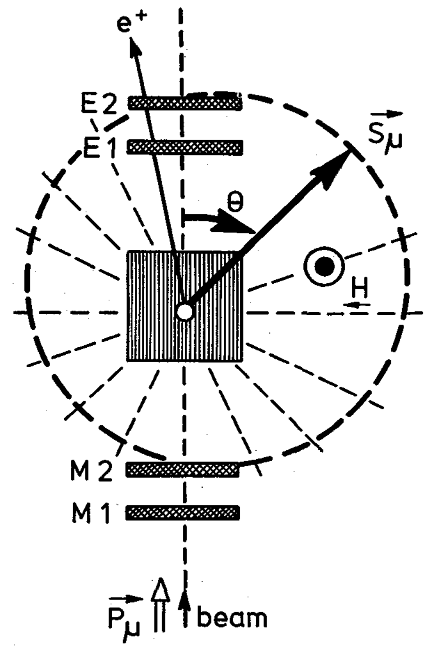

Fig. 1 : Principle arrangement of a μSR-set up in a transverse magnetic field. The detectors M_1 and M_2 serve to identify an incoming muon and the detectors E_1 and E_2 an outgoing positron. The box at the center indicates the target. The dashed circular line represents the asymmetric decay probability distribution with respect to the muon spin $\vec{S}_\mu$.

the decay positron signal and forming a histogram of positron rate versus time. An example for such a histogram is given in figure 2.

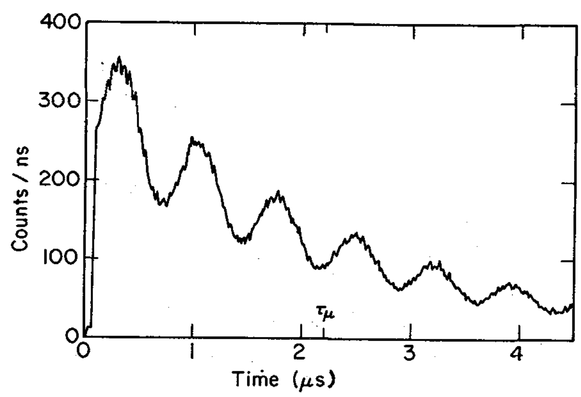

Fig. 2 : Typical experimental histogram for muons precessing in a transverse field of 100 gauss.

The positron rate can be expressed as

$$N_{e^+}(t) = N_o e^{-t/\tau_\mu}(1+A\, P(t)\cos(\omega_\mu t+\psi)) + B \qquad (1)$$

with B = time independent background, τ_μ = average lifetime of μ, ω_μ = Larmor precession frequency, ψ = a phase, determined by the position of the e^+-telescope, A = effective decay asymmetry, and P(t)= damping function, which describes some possible depolarization.

The measurement of ω_μ will determine the actual field at the muon site (external + internal fields, e.g. hyperfine fields, Knight shifts etc.). P(t) will be the result of a static field spread in the target and/or of dynamical relaxation-processes.

It is evident that the muon spin rotation (μSR) technique is analogous to the free precession decay technique in NMR (being the Fourier transform of the usual line shape measurements) and to the nuclear methods of angular correlation and distribution measurements.

In the case of a static field spread the damping function can be approximated by $P(t) = \exp(-\sigma^2 t^2)$ (inhomogeneous line broadening in NMR), while for dynamical relaxation $P(t) = \exp(-{}^{t}/T_2)$ (homogeneous line broadening in NMR). A static field spread could e.g. originate from nuclear dipole fields in which instance σ^2 is related to the 2nd moment of the dipolar field spread (Van Vleck theory, see e.g. reference /9/).

3. POSITIVE MUONS IN METALS : DIFFUSION, LOCALIZATION AND TRAPPING AT IMPURITIES.- Diffusion studies are possible in those cases where an internal static field spread is present (either of nuclear or electronic origin) and where the motion of the muon can then lead to a motional slowing down of the depolarization rate, the analogue of motional line narrowing in NMR. The damping function in the presence of diffusion is very well approximated by /9/

$$P(t) = \exp\left[-\sigma^2 \tau_c^2 \left\{\exp(-{}^{t}/\tau_c) - 1 + {}^{t}/\tau_c\right\}\right] \quad (2)$$

where τ_c is a correlation time that can be identified with the average residence time at some interstitial position and σ^2 is related to the second moment of the internal field spread (see also reference /10,11/).

The diffusion of muons has been observed for the first time by Grebinnik et al. /12/ in copper. The results of some more recent measurements /13/ in single crystal of Cu are shown in figure 3. Plotted is the damping rate λ, defined by $P(1/\lambda) = 1/e$, as a function of temperature. One recognizes a plateau- and a motional slowing down region. In the plateau region the jump rate of the muon is very small and λ can be identified with σ^2. From the slowing down region the temperature dependence of the jump rate τ_c^{-1} can be obtained, shown in figure 4 in a semilogarithmic plot. The data are nicely

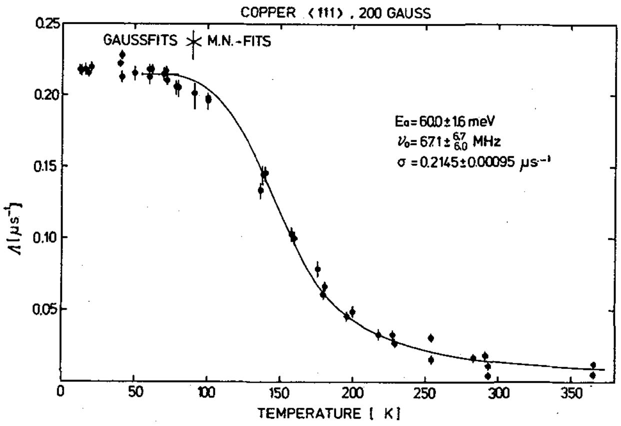

Fig. 3 : Damping rate λ for muons in Cu versus temperature. The solid line represents a simultaneous fit to all histograms.

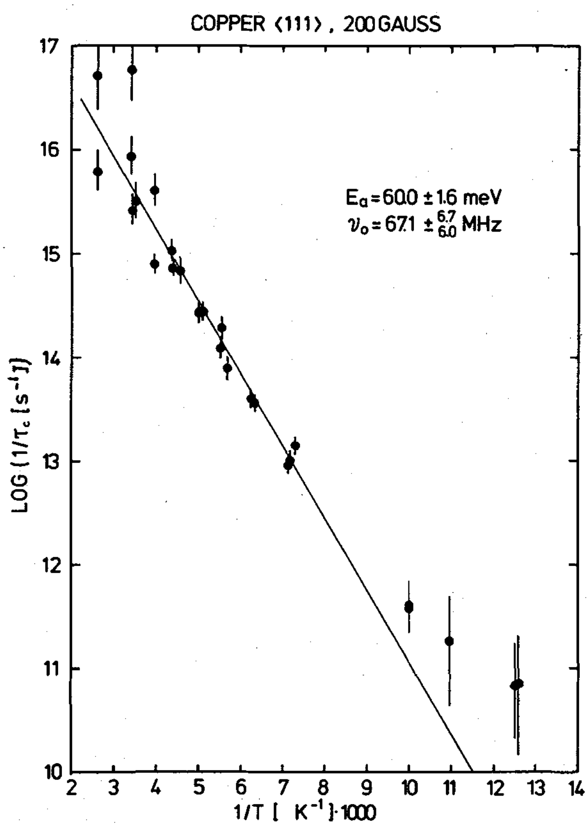

Fig. 4 : Plot of the fitted hoppingrate τ_c^{-1} versus temperature for muons in Cu. The solid line represents a fit of equation 3 to these data /13/.

described by an Arrhenius relationship

$$\frac{1}{\tau_c} = \nu_o \exp\left(-\frac{E_a}{kT}\right) \quad (3)$$

where E_a is an activation energy. The fitted pre-exponential factor is about four orders of magnitude smaller than the corresponding value for hydrogen, obtained at much higher temperature though.

This has been interpreted as evidence for a sub barrier quantum tunnelling diffusion below room temperature /12,14/.

Analysis of the low temperature value for σ^2 and its change with crystal orientation allowed a determination of the site of localization (octahedral interstitial site) and of the lattice dilatation (~ 5 %) around the muon /15/. The overall picture which emerges is that of a self trapped muon, the activation energy of its diffusion being related to the lattice relaxation energy /16/ and the diffusion being that of a small polaron which tunnels by phonon assistance randomly from site to site /7/.

A new phenomenon is encountered in the data obtained in a high purity single crystal of Niobium /17/. The results for λ are shown in figure 5.

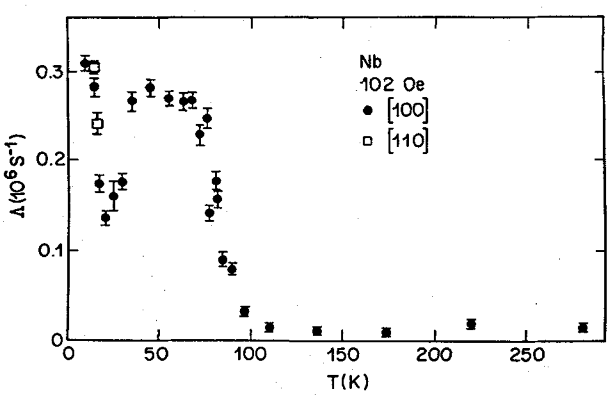

Fig. 5 : Damping rate λ for muons in Nb versus temperature. The crystal axis assignments denote that the external field was oriented parallel to these axes /17/.

A surprising feature is the quite deep dip around 20 K, extending over only about 15 K temperature range. The structure of the dip has been investigated in the presence of various amounts of interstitial O, N, C and H impurities /18/. High impurity concentrations lead to a disappearance of the dip. The data have been explained in terms of a two stage diffusion process /17,18/. At the lowest temperatures the muon seems to be selftrapped at tetrahedral interstitial sites, perhaps being in an extended (tunnelling) state over several neighboring interstitial sites. With increasing temperature the intrinsic interstitial diffusion is observed, leading to a rapid motional slowing down (left side of the dip). With further increasing temperature the intrinsic motions become fast enough so that the muon can reach an impurity trap during its life time, where it is frozen in again. This leads to the second plateau region. Only at still higher temperatures one begins to observe the escape from the trap, leading to the second motional slowing down region.

The general features of the Nb-data are not unique. Complicated structures have also been found in Bi /19/, Ta /20/ and V /21,22,23/ at relatively low temperatures. As an example figure 6 shows some recent data obtained in single crystals of V /23/.

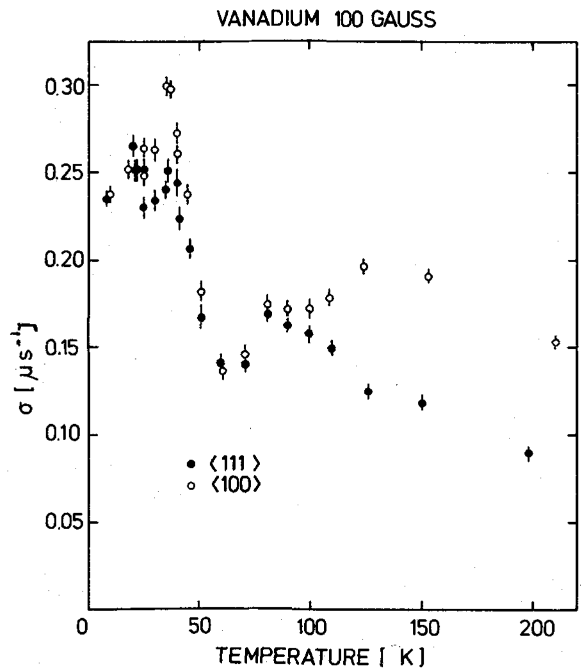

Fig. 6 : Damping rate λ for muons in V versus temperature for two crystal orientations with respect to the applied field /23/.

One recognizes a dip and a peak and even more complicated structure, when the <111>-crystal axis was oriented parallel to the external magnetic field.

One of the main motivations of muon diffusion studies is the detection and study of quantum effects, which because of the much lighter mass of the muon, may be more successfull with muons than with protons. So far unambiguous clear evidence for quantum effects is lacking or only marginal. In view of this, very low temperature studies of μ^+-diffusion (i.e. much below 4 K) are certainly a very promising path of future research, which, for various reasons, does not seem to be open to the conventional methods of hydrogen diffusion investigations.

4. MAGNETIC STUDIES.-

4.1. Internal Magnetic Fields in Ferromagnetic Co and Antiferromagnetic α-Fe_2O_3.- μSR-results in these two substances will be discussed as a representative example. There are no particular low temperature aspects in these data, but the results are suggestive of what could be done in other magnetic compounds at low temperature.

The internal field at a positive muon is generally composed of the following contributions

$$\vec{B}_\mu = \vec{B}_{ext} + \vec{B}_{dem} + \vec{B}_L + \vec{B}_{dip} + \vec{B}_{hf} \quad (4)$$

where $\vec{B}_{ext}$ = external magnetic field, $\vec{B}_{dem}$ = demagnetization field, $\vec{B}_L$ = Lorentz field, $\vec{B}_{dip}$ = field from dipoles within the Lorentz sphere and $\vec{B}_{hf}$ = contact hyperfine field due to the conduction electrons. The latter is of course only present in metals.

Figure 7 shows results for B_μ obtained in a single crystal of Co as a function of temperature /24/. At low temperature the internal field is first

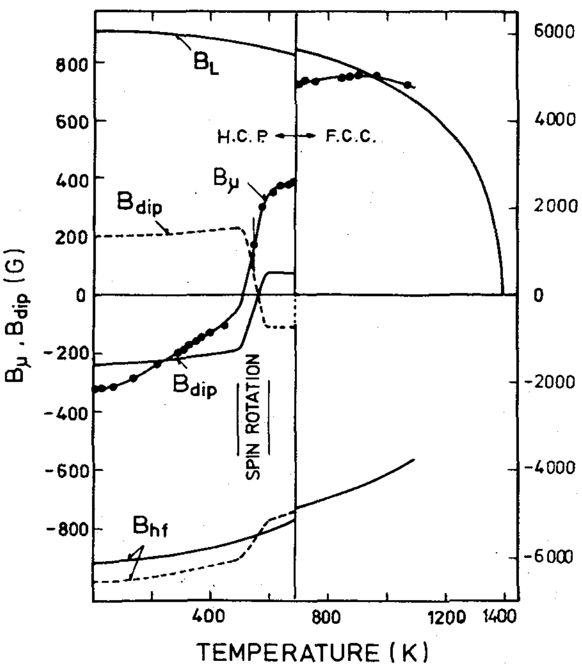

Fig. 7 : Temperature dependence of the local field B_μ in cobalt in zero applied field. Shown are also the calculated dipolar fields (projected on the local magnetization direction for different site assignments of the μ^+. Solid : octahedral, dashed = tetrahedral), the Lorentz field B_L and the hyperfine field B_{hf}. Only the octahedral site assignment leads to a smooth temperature dependence of B_{hf} /24/.

negative, decreasing smoothly in magnitude with increasing temperature up to 450 K. In this temperature region the easy axis of magnetization is along the hexagonal c-direction. In the temperature range 500 - 600 K the internal field changes quite abruptly its sign. This behavior happens in parallel to a rotation of the easy axis of magnetization from the c-direction into the basal plane, as is known from neutron diffraction experiments. At 690 K there is a sudden jump of the value of B_μ by almost a factor of two. At this temperature a phase transition from hcp- to fcc-crystal structure takes place. It is this sensitivity of the muon probe to changes of magnetic properties which could make it attractive also for low temperature investigations. Another example in this respect is shown in figure 8. It shows the temperature dependence of B_μ in the antiferromagnetic insulator α-Fe_2O_3 /25/. At 263 K

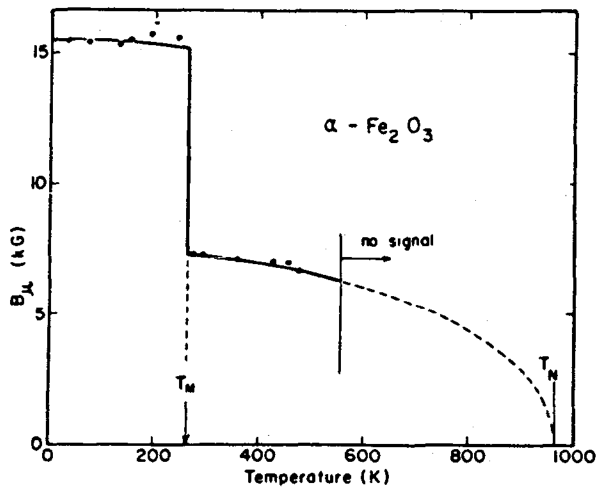

Fig. 8 : Temperature dependence of the local field B_μ in α-Fe_2O_3 in zero applied field. Above 500 K the local field is averaged to zero due to rapid μ^+ diffusion /25/.

the field is seen to drop abruptly in magnitude. This temperature (called Morin temperature) corresponds to a magnetic phase transition where the spontaneous sublattice magnetization changes from being parallel to the trigonal c-axis to lying in planes perpendicular to this axis.

4.2 Investigations in Spin Glasses and Giant Moment Alloys.- The first spin glasses investigated by μSR were the alloys <u>Cu</u> Mu (0.7 %) and <u>Au</u> Fe (1.5 %) /26/. The aim was to measure the static local magnetic field distribution associated with the spin glass ordering (T_c(<u>Cu</u> Mu) = 7.7 K, T_c (<u>Au</u> Fe) = 11.6 K). Local magnetic fields at the muon position can originate from the electronic magnetic moments, and from the contact hyperfine interaction with the conduction electrons which are spin polarized by the RKKY interaction. Figure 9 shows the experimental results for the static field spread Δ, obtained from the observed damping rate T_2^{-1} by the relation $\Delta = (\gamma_\mu T_2)^{-1}$. The field spread above the ordering temperature is very small and is caused by the nuclear magnetic dipoles. Around and below the transition temperature the field spread increases abruptly, being more sharp in small applied external magnetic fields. This points to a field induced spin freezing already above T_c. The abrupt appearance of large local field inhomogeneities at the ordering temperature indicates that a real magnetic phase transition takes place in accordance with the mean field theory of spin freezing while the absence of a gradual onset of local ordering disproves random-molecular-field theories /26/. The observed low temperature field spread is in agreement with estimates from the theory of reference /27/, which rules out the existence of static conduction electron spin density waves and the existence of a finite probability density of zero molecular field /26/.

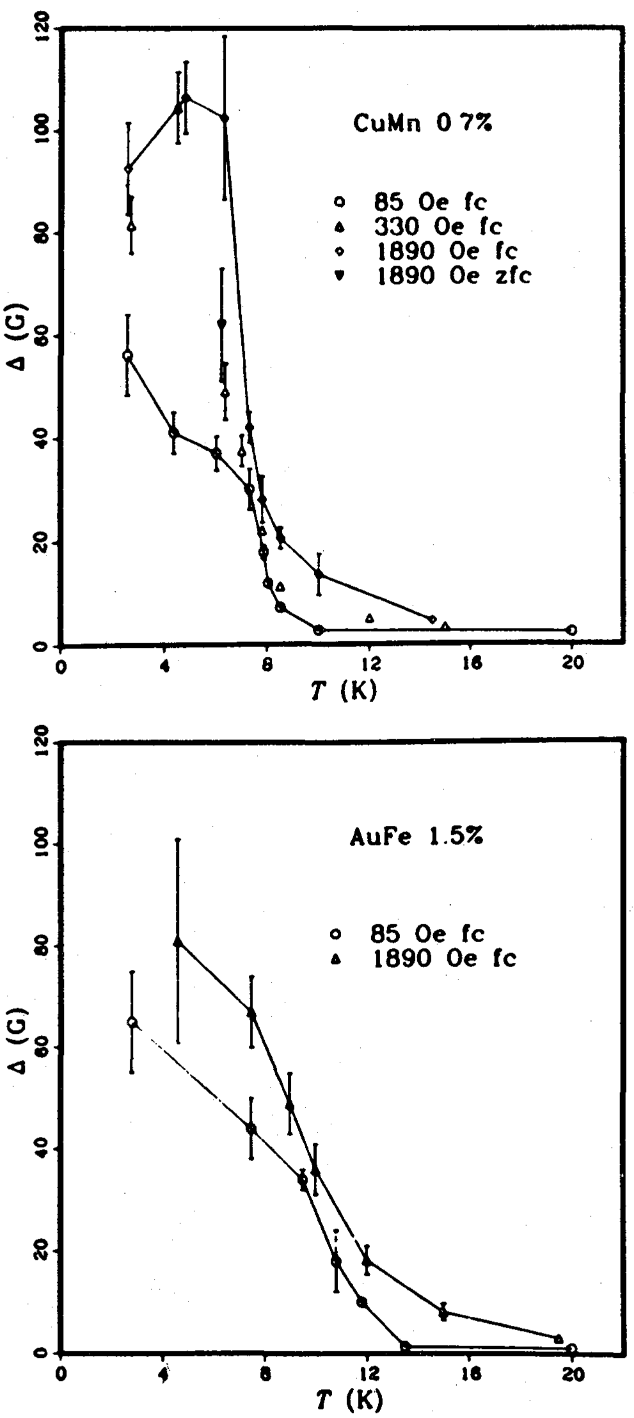

Fig. 9 : Temperature dependence of depolarization rate, expressed as a line width, in Cu Mn and Au Fe for several values of the applied magnetic field /26/. T_c is 7.7 K for Cu Mn and 11.6 K for Au Fe.

Similar results were found in the giant moment alloys Pd Fe (0.015 - at %) and Pd Fe (0.28 - at %) /28/. The more iron rich alloy orders ferromagnetically at 9.0 K while the very dilute Pd Fe alloy shows an antiferromagnetic or spin glass ordering around 0.4 K, according to susceptibility measurements. The difference in magnetic behavior is clearly visible in the μSR-data, figure 10. For

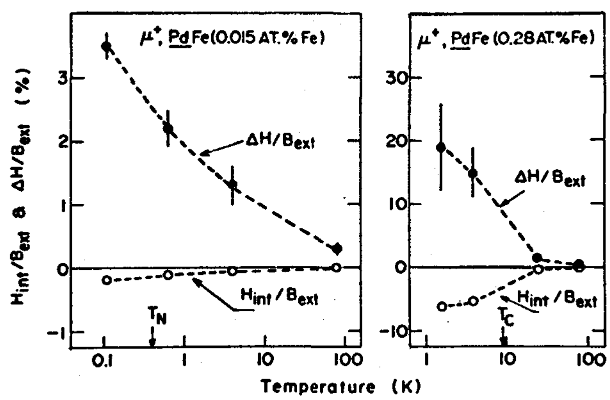

Fig. 10 : Temperature dependence of depolarization rate, expressed as a relative line width $\Delta H/B_{ext_1}$ in two Pd Fe alloys. Also shown is the temperature dependence of the hyperfine field B_{hf}.

Pd Fe (0.28 - at %) one observes at T_c an abrupt increase in local field spread while the data in Pd Fe (0.015 - at %) show a very gradual increase of the field spread with decreasing temperature when passing over the transition temperature. The absence of a sharp transition in the latter case may be due to the relatively large external magnetic field of 1 kG causing a spin freezing already above 0.4 K or, perhaps, may point to the absence of a real phase transition.

A gradual spin freezing has been indeed observed by μSR in the insulator spin glass Mn $O \cdot Al_2O_3 \cdot SiO_2$ /29/. Figure 11 shows the muon depolarization rate versus temperature. The high tem-

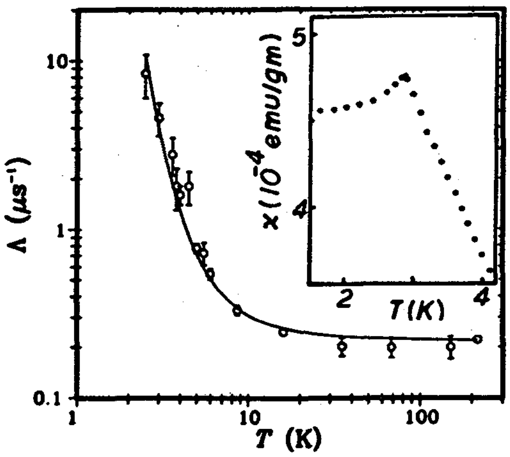

Fig. 11 : Temperature dependence of the depolarization rate λ in $MnO \cdot Al_2O_3 \cdot SiO_2$. The inset shows the low field, AC susceptibility of one small piece out from the target sample /29/.

perature damping rate is again due to nuclear dipole fields. The low temperature damping rate, on the other side, increases quickly with decreasing temperature and can be fitted nicely with an Arrhenius type of expression. This increase is attributed to Mn electronic spins and is explained in terms of a super paramagnetic domain model /29/. According to this model the electronic spins are magnetically ordered in small domains with a diameter of typically 12 Å, possessing a net magnetic moment and fluctuating thermally in their orientation. A magnetic phase transition is definitely not indicated by the data. The electronic correlation times, extracted from the present μSR-data, are inconsistent with corresponding results from low field AC susceptibility measurements.

4.3. Magnetic Effects in Superconducting Metals.- For completeness some measurements have to be mentioned here that have been performed in type I and type II superconductors. In lead one has found that muons stop to precess below the transition temperature /30/, which is a nice demonstration of the Meissner effect. In Nb and a Pb In-alloy one has tried to probe the superconducting vortex structure in the mixed state /31/. The results are not very instructive due to the limited accuracy of the data and due to problems arising form the mobility of the muons at these low temperatures.

5. CONCLUSION.- Various examples of the application of the μSR technique have been presented. Low temperatures were in most cases a necessary experimental condition. The results do indicate, without doubt, that the μSR-technique could be an important tool also in low temperature physics.

References

/1/ Brewer,J.H., Crowe,K.M., Gygax,F.N. and Schenck, A., in Muon Physics, ed. by V.W. Hughes and C.S. Wu (Academic Press) 1975, vol III

/2/ Schenck,A., in Nuclear and Particle Physics at Intermediate Energy, ed. by J.B. Warren (Plenum Publ.) 1976

/3/ Garwin,R.L., Ledermann,L.M. and Weinrich,M., Phys. Rev. 105 (1957) 1415

/4/ a) Proceedings of Fourth International Conference on Hyperfine Interactions, published in Hyperf. Int. 4 (1978) 1-986
b) Proceedings of First International Topical Meeting on μSR, Rorschach, Sept. 4 - 7, 1978 to be published

/5/ See e.g. Seeger,A., in Hydrogen in Metals, ed. by G. Alefeld and J. Völkl, to be published

/6/ See e.g. Schenck,A., Hyperf. Interact. 4 (1978) 228

/7/ Flynn,C.P. and Stoneham,A.M., Phys. Rev. B1 (1970) 3966
Kagan,Yu. and Klinger,M.I., J. Phys. C7 (1974) 2791
Stoneham,A.M., J. Nucl. Mater. 69 & 70 (1978) 109

/8/ Spin polarized muon beams are formed from pions decaying in flight or at rest. In the rest frame of the pions positive muons are 100 % spin polarized opposite to their momentum. This is also a consequence of parity violation in the weak decay of the pion (see e.g. reference /1/)

/9/ Abragam,A., The Principles of Nuclear Magnetism, (Clarendon, Oxford) 1970

/10/ Baryshevskii,V.G. and Kuten,S.A., Sov. Phys. Solid State 18 (1977) 1677

/11/ McMullen,T. and Zaremba,E., to be published

/12/ Grebinnik,V.G. et al., Sov. Phys. JETP 41 (1976) 777

/13/ Schilling,H. et al., see reference 4 b)

/14/ Teichler,H., Phys. Lett. 64A (1977) 78

/15/ Camani,M. et al., Phys. Rev. Lett. 39 (1977) 836

/16/ Teichler,H., to be published (see also reference 4 b)

/17/ Birnbaum,H.K. et al., Phys. Lett. 65A (1978) 435

/18/ Borghini,M. et al., Phys. Rev. Lett. 40 (1978) 1723

/19/ Grebinnik,V.G. et al., Pisma Ztz. Eksp. Teor. Fiz. 25 (1977) 322

/20/ Herlach,D. et al. (see reference 4 b)

/21/ Hartmann,O. et al., Hyperf. Interact. 4 (1978) 824

/22/ Fiory,A.T. et al., Phys. Rev. Lett. 40 (1978) 968

/23/ Schilling,H. et al., (see reference 4 b)

/24/ Graf,H. et al., Phys. Rev. Lett. 37 (1976) 1644

/25/ Graf,H. et al., Hyperf. Interact. 4 (1978) 452

/26/ Murnick,D.E., Phys. Rev. Lett. 36 (1976) 100

/27/ Walstedt,R.E. and Walker,L.R., Phys. Rev. B9 (1974) 4857

/28/ Nagamine,K. et al., Phys. Rev. Lett.38 (1977) 99

/29/ Bieman,L.H. et al., Hyperf. Interact. 4 (1978) 861

/30/ Crowe,K.M. et al., unpublished data, see also reference 1

/31/ Fiory,A.T. et al., Phys. Rev. Lett 33 (1974) 969